投稿論文(英文)
PAPERS

Proc. of JSCE No. 467/II-23, pp. 103~113, May 1993

EVALUATION OF OPEN CHANNEL FLOW WITH VARYING ASPECT RATIO AND ROUGHNESS RATIO

Yongdi YANG* and Atsuyuki DAIDO**

A flow pattern with varying aspect ratio (breadth/depth) and boundary roughness ratio (bed roughness/ side wall roughness) in open channel is proposed in this paper. The distribution of boundary shear and the mean boundary shear are studied. On the basis of this, velocity distribution and flow resistance are further discussed. The evaluation formulae of boundary shear, velocity distribution and flow resistance are derived systematically. The results are suitable for all aspect ratio and roughness ratio, and are better in agreement with a wide range of experimental data. These are much helpful to the study of sediment transport, flow diffusion, river engineering, etc.

Key Words: *open channel flow, boundary shear stress, velocity distribution, resistance coefficient, aspect ratio, roughness*

1. INTRODUCTION

The evaluation of open channel flow with varying aspect ratio (breadth/depth) and roughness ratio (bed roughness/side wall roughness) is an essential problem in the study of three-dimensional flow structure, and is of great importance to sediment transport, river engineering and hydraulic model experiments. With the variation of aspect ratio and roughness ratio, the flow structure, resistance and boundary shear are quite different. In general, the flow structure has three-dimensional characteristics, the resistance depends on the roughness of all the walls, and the distribution of boundary shear along the wetted perimeter is non-uniform. Experimental data[1)~3)] show that secondary flow takes place near the corner of bed and side wall due to the side wall influence. This causes momentum transport and suspended material diffusion in transverse direction. Thus it is necessary to precisely evaluate the effect of varied aspect ratio and roughness ratio upon the flow.

Traditional studies on the evaluation of open channel flow are mostly carried out individually in flow resistance[4),9)], boundary shear, etc.[5),7),20)], such as the empirical method of partition of water cross sectional area[23)], and the diagrammatic method to evaluate the boundary shear distribution on the bed[21)]. As resistance, velocity distribution and boundary shear are all the variables of open channel flow, there must be some relationships among them. In this paper, an evaluation method of open channel flow is established.

* Member of JSCE, M. Eng., Graduate Student, Dept. of Civil Eng., Ritsumeikan Univ., (56-1, Kitamachi, Tojin Kitaku, Kyoto 603)
** Member of JSCE,Dr.Eng., Prof., Ritsumeikan Univ.

Based on the previous studies[7)~10)], a flow pattern for varying aspect ratio and roughness ratio is set up. The boundary shear distribution, and the flow characteristics with different aspect ratio and roughness ratio are discussed. A systematic method to evaluate boundary shear, velocity distribution and flow resistance is proposed. The comparison between the present results and a wide range of experimental data shows good agreement.

2. FLOW PATTERN AND BASIC EQUATIONS

(1) Two types of open channel flow

It is generally thought that when aspect ratio is very large, the side wall influence upon open channel flow can be ignored, and the flow is regarded as two-dimensional approximately. With the decrease of aspect ratio, the side wall influence becomes greater and the three-dimensional characteristics appear, and when aspect ratio is very small, the flow mainly depends on the side wall, and the bed effect can be ignored, then the flow can be considered as two-dimensional one between two side walls. Hence, with the variation of aspect ratio, the flow tends to two different extremes, one is the two-dimensional flow on the bed, while the other is the two-dimensional flow between two side walls.

An experiment was carried out in a plate flume, 14300 mm in length, 132 mm in width and 750 mm in depth. The velocity and turbulence intensity were measured with the aspect ratio of 0.107. The side wall of flume was made of sand (Δ_s=1.6 mm), the bed of steel plate. The velocity was measured with a micro-propeller velocity meter (ϕ=3 mm). **Fig.1** and **Fig.2** are measured distributions of velocity and turbulence intensity normal to the side

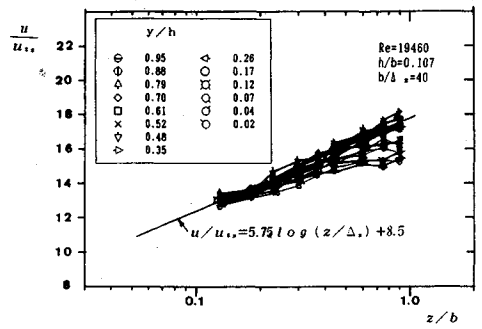

Fig.1 Velocity distribution normal to side wall.

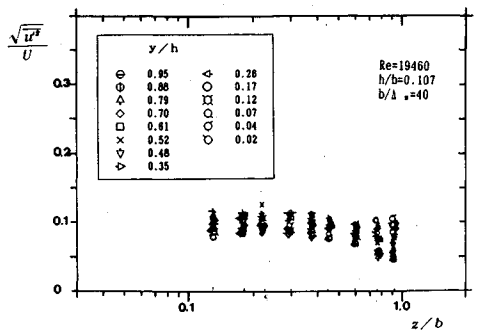

Fig.2 Turbulence intensity distribution normal to side wall.

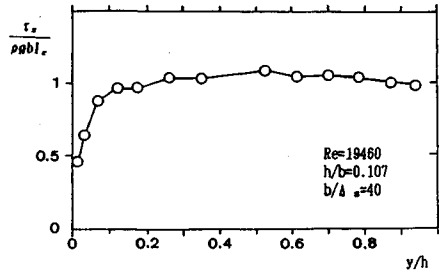

Fig.3 Boundary shear distribution along side wall.

wall in the half cross section. Compared with the velocity and turbulence intensity at half water depth, the velocity and turbulence intensity are decreased and increased respectively near the bed, and both decreased near the water surface. In other regions, the velocity distribution conform to Nikuradse-Prandtl's logarithmic law, i.e.

$$\frac{u}{u_{*s}}=5.75\log\left(\frac{z}{\Delta_s}\right)+8.5 \quad \cdots\cdots(1)$$

where u=velocity, u_{*s}=shear velocity related to side wall, $u_{*s}=\sqrt{gbI_e}$, b=half width, I_e=energy slope, g=gravity acceleration, Δ_s=side wall roughness height. In **Fig.2**, $\sqrt{\overline{u^{12}}}$=turbulence intensity, U=mean velocity in cross section.

Fig.3 is the boundary shear distribution along the side wall with shear derived from velocity

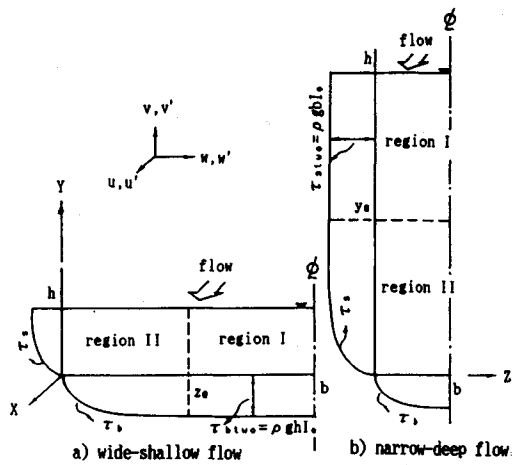

Fig.4 Two types of open channel flow.

distribution. The figure shows that the boundary shear stress near the bed is reduced.

The results indicate that the open channel flow with small aspect ratio agree with two-dimensional characteristics except in the regions near the bed and the water surface.

Thus for varying aspect ratio, the open channel flow can be divided into two types as demonstrated in **Fig.4**. One is wide-shallow flow which mainly depends on the bed (**Fig.4** a), while the other is narrow-deep flow which mainly depends on the side wall (**Fig.4** b).

(2) Basic equations

As mentioned above, the two-dimensional flow is not influenced by side wall only when the aspect ratio is very large. In order to analyze the characteristics of open channel flow in general, the cross section is divided into two regions, i.e. the two-dimensional flow region (region Ⅰ) and the mixed flow region (region Ⅱ) as shown in **Fig.4**.

The motion equations for steady uniform flow in x direction are discussed. In the two-dimensional flow region, the influence of the wall which the flow dose not touch is so small that can be ignored. The motion equations can be written as：

$$g\sin\theta-\frac{1}{\rho}\frac{dp}{dx}+\frac{d}{dy}\left(-\overline{u'v'}+\nu\frac{du}{dy}\right)=0$$

for wide-shallow flow ····· (2a)

$$g\sin\theta-\frac{1}{\rho}\frac{dp}{dx}+\frac{d}{dz}\left(-\overline{u'w'}+\nu\frac{du}{dz}\right)=0$$

for narrow-deep flow····· (2b)

In the mixed flow region, both side wall and bed influences exist, the secondary flow in the cross section occurs and the shear stress in two directions appear. The motion equations are written as：

$$\frac{\partial v}{\partial y}+\frac{\partial w}{\partial z}=0$$

$$v\frac{\partial u}{\partial y}+w\frac{\partial u}{\partial z}=g\sin\theta-\frac{1}{\rho}\frac{\partial p}{\partial x}+\frac{\partial}{\partial y}\left(-\overline{u'v'}+\nu\frac{\partial u}{\partial y}\right)+\frac{\partial}{\partial z}\left(-\overline{u'w'}+\nu\frac{\partial u}{\partial z}\right)$$

$$v\frac{\partial v}{\partial y}+w\frac{\partial v}{\partial z}=-g\cos\theta-\frac{1}{\rho}\frac{\partial p}{\partial y}+\frac{\partial}{\partial y}\left(-\overline{v'v'}+\nu\frac{\partial v}{\partial y}\right)+\frac{\partial}{\partial z}\left(-\overline{v'w'}+\nu\frac{\partial v}{\partial z}\right)$$

$$v\frac{\partial w}{\partial y}+w\frac{\partial w}{\partial z}=-\frac{1}{\rho}\frac{\partial p}{\partial z}+\frac{\partial}{\partial y}\left(-\overline{wv}+\nu\frac{\partial w}{\partial y}\right)+\frac{\partial}{\partial z}\left(-\overline{ww}+\nu\frac{\partial w}{\partial z}\right)\quad\cdots\cdots(3)$$

where u, v, w are time-averaged velocity and u', v' w' are velocity fluctuation in x, y, z directions respectively, p=average pressure, ν=kinematic viscosity, θ=bed slope, h=depth, ρ=water density.

The shear stress is expressed as,

$$\left.\begin{aligned}\frac{\tau_{xy}}{\rho}&=-\overline{u'v'}+\nu\frac{\partial u}{\partial y}\\ \frac{\tau_{xz}}{\rho}&=-\overline{u'w'}+\nu\frac{\partial u}{\partial z}\end{aligned}\right\}\quad\cdots\cdots(4)$$

The energy slope is,

$$I_e=\sin\theta-\frac{1}{\rho g}\frac{\partial p}{\partial x}\quad\cdots\cdots(5)$$

For wide-shallow flow, substituting Eqs.(4) and (5) into Eqs.(2a) and (3), and then integrating them, we have,

$$\frac{\tau_{xy}}{\rho}=gI_eh\left(1-\frac{y}{h}\right)-\int_y^h\left(\frac{\partial uv}{\partial y}+\frac{\partial uw}{\partial z}\right)dy+\int_y^h\frac{\partial}{\partial z}\left(\frac{\tau_{xz}}{\rho}\right)dy\qquad 0\leqq z\leqq z_0$$

$$\frac{\tau_{xy}}{\rho}=gI_eh\left(1-\frac{y}{h}\right)\qquad z_0\leqq z\leqq b$$

$$\frac{\tau_{xz}}{\rho}=gI_ez_0\left(1-\frac{z}{z_0}\right)-\int_z^{z_0}\left(\frac{\partial uv}{\partial y}+\frac{\partial uw}{\partial z}\right)dz+\int_z^{z_0}\frac{\partial}{\partial y}\left(\frac{\tau_{xy}}{\rho}\right)dz\qquad 0\leqq z\leqq z_0\quad\cdots(6)$$

Let τ_b be the boundary shear on the bed, and τ_s be the boundary shear on the side wall, then

$$\left.\begin{aligned}\frac{\tau_b}{\rho}&=gI_eh-\frac{d}{dz}\int_0^h\left(uw-\frac{\tau_{xz}}{\rho}\right)dy\qquad 0\leqq z\leqq z_0\\ \frac{\tau_b}{\rho}&=gI_eh\qquad z_0\leqq z\leqq b\\ \frac{\tau_s}{\rho}&=gI_ez_0-\frac{d}{dy}\int_0^{z_0}\left(uv-\frac{\tau_{xy}}{\rho}\right)dz\qquad 0\leqq z\leqq z_0\end{aligned}\right\}\quad\cdots(7)$$

The mean boundary shear on the bed and the side wall are defined as,

$$\left.\begin{aligned}\overline{\tau_b}&=\frac{1}{b}\int_0^b\tau_b dz\\ \overline{\tau_s}&=\frac{1}{h}\int_0^h\tau_s dy\end{aligned}\right\}\quad\cdots\cdots(8)$$

integrating Eq.(7) from $z=0$ to $z=b$, we obtain:

$$b\overline{\tau_b}+h\overline{\tau_s}=(b+h)\tau_0\quad\cdots\cdots(9)$$

where $\tau_0=\rho gRI_e$, R is hydraulic radius, $R=hb/(h+b)$.

The relationship similar to Eqs.(6-9) can also be obtained for the narrow-deep flow in the same way.

(3) The range of mixed flow region

As to the wide-shallow flow, Sawano et al.[20] found from experimental data that the range of mixed flow region was 2.1 times the water depth in average, i.e. $z_0/h=2.1$. For non-uniform roughness, the range of mixed flow region is related to roughness ratio, and assumed to be,

$$\frac{z_0}{h}=a\left(\frac{\Delta_s}{\Delta_b}\right)^\alpha\quad\cdots\cdots(10a)$$

The coefficient a and exponent α are determined by experimental data.

For the narrow-deep flow, the range of mixed flow region is obtained in the same way.

$$\frac{y_0}{b}=a\left(\frac{\Delta_b}{\Delta_s}\right)^\alpha\quad\cdots\cdots(10a)$$

The critical point to distinguish wide-shallow flow from narrow-deep flow falls between $\frac{1}{a}\left(\frac{\Delta_s}{\Delta_b}\right)^\alpha$ and $a\left(\frac{\Delta_s}{\Delta_b}\right)^\alpha$, and can be written as,

$$\left(\frac{b}{h}\right)_c=\gamma\left[\frac{1}{a}\left(\frac{\Delta_s}{\Delta_b}\right)^\alpha+a\left(\frac{\Delta_s}{\Delta_b}\right)^\alpha\right]\quad\cdots\cdots(11a)$$

where $(b/h)_c$ is the critical value of width-depth ratio to distinguish wide-shallow flow from narrow-deep flow, γ being a constant. On the other hand, the critical value of depth-width $(h/b)_c$ can also be written as,

$$\left(\frac{h}{b}\right)_c=\gamma\left[a\left(\frac{\Delta_b}{\Delta_s}\right)^\alpha+\frac{1}{a}\left(\frac{\Delta_b}{\Delta_s}\right)^\alpha\right]\quad\cdots\cdots(11b)$$

The solution simultaneously satisfying Eq.(11a) and Eq.(11b) is,

$$\gamma=\frac{a}{1+a^2}$$

Therefore, the criteria are as follows:

$$\left.\begin{aligned}\frac{b}{h}&\geqq\left(\frac{\Delta_s}{\Delta_b}\right)^\alpha\quad\text{for wide-shallow flow}\\ \frac{b}{h}&\leqq\left(\frac{\Delta_s}{\Delta_b}\right)^\alpha\quad\text{for narrow-deep flow}\end{aligned}\right\}\quad\cdots\cdots(12)$$

3. EVALUATION OF BOUNDARY SHEAR STRESS

Eq.(6) shows that the boundary shear stress is

related to the secondary flow. A large quantity of experimental data reveal that the secondary flow velocity is 2~3% of the main flow velocity[2),3)]. Due to the existence of the secondary flow, the momentum is transmitted in the cross section, resulted in the non-uniformity of boundary shear distribution[3),11),20)]. As the secondary flow is very complex and difficult to analyze in theory, the method for evaluating boundary shear has not yet well been established. In this paper, the boundary shear formulae for varying aspect ratio and roughness ratio are developed based on experimental data.

(1) Boundary shear distribution

As for the wide-shallow flow shown in **Fig.4**(a), the flow in region I can be approximated as two-dimensional owing to smallness of the side wall influence. The boundary shear depends only on the bed and conforms to uniform distribution. The flow in region II is influenced significantly by the side wall. Therefore the boundary shear depends on both the bed and the side wall and is of non-uniform distribution. If the influence of water surface is ignored, the boundary shear can be written as,

$$\left.\begin{array}{ll}\tau_b=\tau_{btw0} & z_0\leqq z\leqq b\\ \tau_b\left(\frac{z}{z_0}\right)=fn\left(\frac{z}{z_0}\right)\tau_{btw0} & 0\leqq z\leqq z_0\\ \tau_s\left(\frac{y}{h}\right)=fn\left(\frac{y}{h}\right)K_s\tau_{btw0} & 0\leqq y\leqq h\end{array}\right\}\cdots\cdots(13)$$

where fn=distribution function, K_s=coefficient, τ_{btw0}=boundary shear of two-dimensional flow in region I, and $\tau_{btw0}=\rho ghI_e$.

The data measured by Ghosh[11)], Tominaga[3)] and Sawano[20)] show that the rate of variation of boundary shear along the bed is inversely proportional to the distance from the side wall. That is,

$$\frac{dfn\left(\frac{z}{z_0}\right)}{d\left(\frac{z}{z_0}\right)}=\frac{C}{\frac{z}{z_0}+\beta}\cdots\cdots(14)$$

where C and β are the constants to be determined.

The distributions of boundary shear both in region I and region II satisfy the boundary continuity condition, i.e $fn(1)=1$, and there is no flow movement at the common boundary of the side wall and the bed, i.e. $fn(0)=0$. Thus

$$fn\left(\frac{z}{z_0}\right)=\frac{ln\left(1+\frac{1}{\beta}\frac{z}{z_0}\right)}{ln(1+1/\beta)}\cdots\cdots(15)$$

and similarly,

$$fn\left(\frac{y}{h}\right)=\frac{ln\left(1+\frac{1}{\beta}\frac{y}{h}\right)}{ln(1+1/\beta)}\cdots\cdots(16)$$

Therefore Eq.(13) is transformed into,

$$\left.\begin{array}{ll}\frac{\tau_b}{\tau_{btw0}}=1 & z_0\leqq z\leqq b\\ \frac{\tau_b}{\tau_{btw0}}=\frac{ln\left(1+\frac{1}{\beta}\frac{z}{z_0}\right)}{ln(1+1/\beta)} & 0\leqq z\leqq z_0\\ \frac{\tau_s}{\tau_{btw0}}=K_s\frac{ln\left(1+\frac{1}{\beta}\frac{y}{h}\right)}{ln(1+1/\beta)} & 0\leqq y\leqq h\end{array}\right\}\cdots\cdots(17a)$$

where K_s is obtained by substituting Eq.(17 a) into Eq.(9).

$$K_s=\frac{z_0}{h}\frac{1/ln(1+1/\beta)-\beta}{1-[1/ln(1+1/\beta)-\beta]}\qquad\text{for } b\geq z_0$$

$$K_s=\frac{b}{h}\frac{1-[(1+\beta z_0/b)ln(1+b/\beta z_0)-1]/ln(1+1/\beta)}{1-[1/ln(1+1/\beta)-\beta]}\qquad\text{for } b\leq z_0$$

The relationship for the narrow-deep flow as shown in Fig.4(b) is also obtained in the same way.

$$\left.\begin{array}{ll}\frac{\tau_s}{\tau_{stw0}}=1 & y_0\leqq y\leqq h\\ \frac{\tau_s}{\tau_{stw0}}=\frac{ln\left(1+\frac{1}{\beta}\frac{y}{y_0}\right)}{ln(1+1/\beta)} & 0\leqq y\leqq y_0\\ \frac{\tau_b}{\tau_{stw0}}=K_b\frac{ln\left(1+\frac{1}{\beta}\frac{z}{b}\right)}{ln(1+1/\beta)} & 0\leqq z\leqq b\end{array}\right\}\cdots\cdots(17b)$$

K_b is derived from Eq.(9).

$$K_b=\frac{y_0}{b}\frac{1/ln(1+1/\beta)-\beta}{1-[1/ln(1+1/\beta)-\beta]}\qquad\text{for } h\geq y_0$$

$$K_b=\frac{h}{b}\frac{1-[(1+\beta y_0/h)ln(1+h/\beta y_0)-1]/ln(1+1/\beta)}{1-[1/ln(1+1/\beta)-\beta]}\qquad\text{for } h\leq y_0$$

Figs.(5 a-5 f) are the comparisons of Eq.(17) with experimental data for uniform and non-uniform boundary roughness. In terms of the multivariate regression analysis method, $\beta=0.079$, and $a=2$, $\alpha=0.1$ in Eq.(12) are obtained, which are in good agreement with the experimental data.

(2) Mean boundary shear

The mean boundary shear on the side wall and the bed can be obtained by applying above results.

For wide-shallow flow

When $b\geq z_0$

$$\left.\begin{array}{l}\frac{\bar{\tau}_b}{\tau_0}=\left(1+\frac{h}{b}\right)\left\{1-\frac{z_0}{b}\left(\frac{1}{ln(1+1/\beta)}-\beta\right)\right\}\\ \frac{\bar{\tau}_s}{\tau_0}=\left(1+\frac{h}{b}\right)\frac{z_0}{h}\left(\frac{1}{ln(1+1/\beta)}-\beta\right)\end{array}\right\}\cdots\cdots(18a)$$

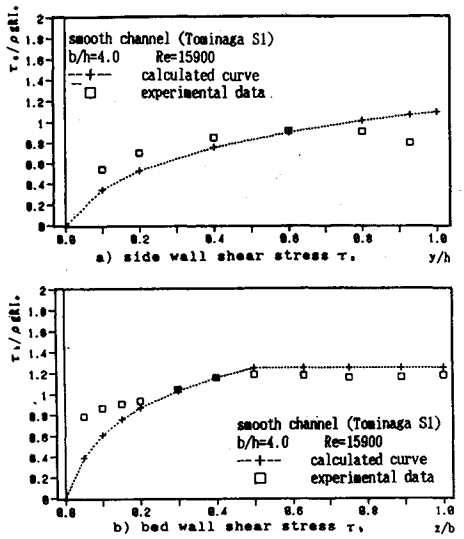

Fig.5(a) Comparison of calculated boundary shear distribution by Eq.(17) with experimental data for smooth wall by Tominaga (S1)[13].

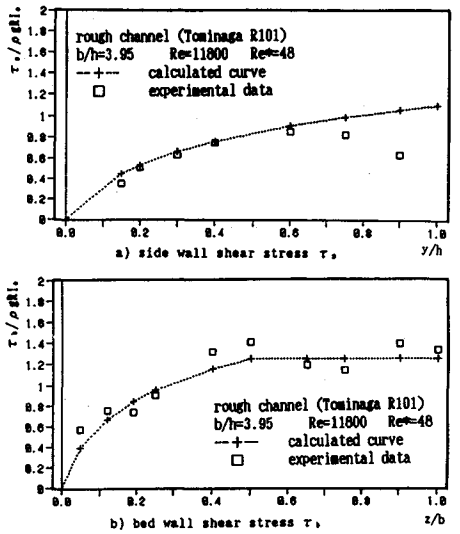

Fig.5(b) Comparison of calculated boundary shear distribution by Eq.(17) with experimental data for uniform boundary roughness by Tominaga(R 101)[13].

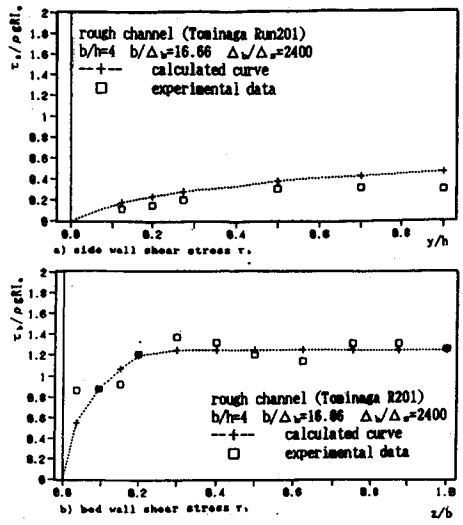

Fig.5(c) Comparison of calculated boundary shear distribution by Eq.(17) with experimental data for non-uniform boundary roughness by Tominaga (R 201)[13].

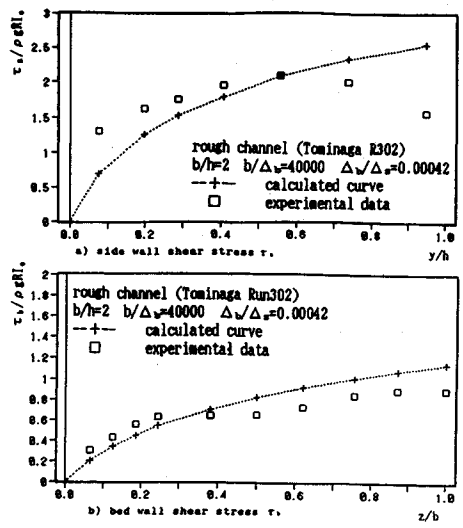

Fig.5(d) Comparison of calculated boundary shear distribution by Eq.(17) with experimental data for non-uniform boundary roughness by Tominaga (R 302)[13].

When $b \leq z_0$

$$\left.\begin{aligned}\frac{\bar{\tau}_b}{\tau_0}&=\left(1+\frac{h}{b}\right)\left\{\left(1+\beta\frac{z_0}{b}\right)\right.\\&\left.\quad ln\left(1+\frac{1}{\beta}\frac{b}{z_0}\right)-1\right\}/ln\left(1+\frac{1}{\beta}\right)\\\frac{\bar{\tau}_s}{\tau_0}&=\left(1+\frac{b}{h}\right)\left\{1-\left[\left(1+\beta\frac{z_0}{b}\right)\right.\right.\\&\left.\left.\quad ln\left(1+\frac{1}{\beta}\frac{b}{z_0}\right)-1\right]/ln(1+1/\beta)\right\}\end{aligned}\right\} \cdots\cdots (18b)$$

For narrow-deep flow

When $h \geq y_0$

$$\left.\begin{aligned}\frac{\bar{\tau}_s}{\tau_0}&=\left(1+\frac{b}{h}\right)\left\{1-\frac{y_0}{h}\left(\frac{1}{ln(1+1/\beta)}-\beta\right)\right\}\\\frac{\bar{\tau}_b}{\tau_0}&=\left(1+\frac{b}{h}\right)\frac{y_0}{b}\left(\frac{1}{ln(1+1/\beta)}-\beta\right)\end{aligned}\right\} \cdots\cdots (18c)$$

When $h \leq y_0$

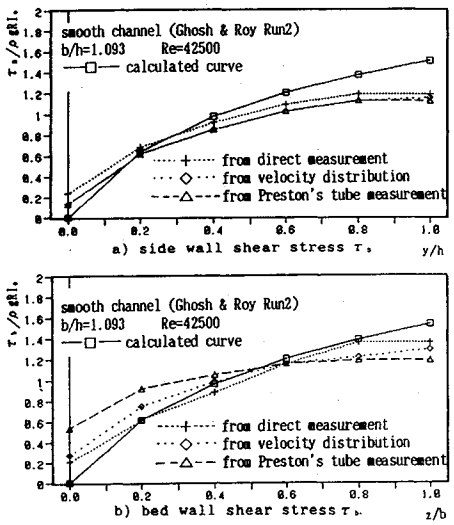

Fig.5(e) Comparison of calculated boundary shear distribution by Eq.(17) with experimental data for smooth wall by Ghosh (Run 2)[11].

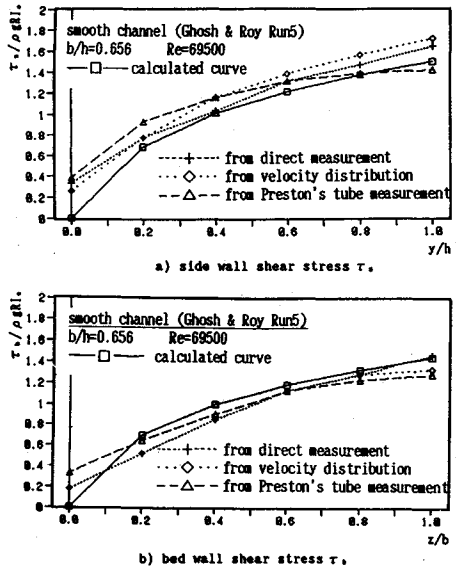

Fig.5(f) Comparison of calculated boundary shear distribution by Eq.(17) with experimental data for smooth wall by Ghosh (Run 5)[11].

$$\left.\begin{aligned}\frac{\bar{\tau}_s}{\tau_0}&=\left(1+\frac{b}{h}\right)\left\{\left(1+\beta\frac{y_0}{h}\right)\right.\\&\left.ln\left(1+\frac{1}{\beta}\frac{h}{y_0}\right)-1\right\}/ln\left(1+\frac{1}{\beta}\right)\\\frac{\bar{\tau}_b}{\tau_0}&=\left(1+\frac{h}{b}\right)\left\{1-\left[\left(1+\beta\frac{y_0}{h}\right)\right.\right.\\&\left.\left.ln\left(1+\frac{1}{\beta}\frac{h}{y_0}\right)-1\right]/ln(1+1/\beta)\right\}\end{aligned}\right\}\cdots(18d)$$

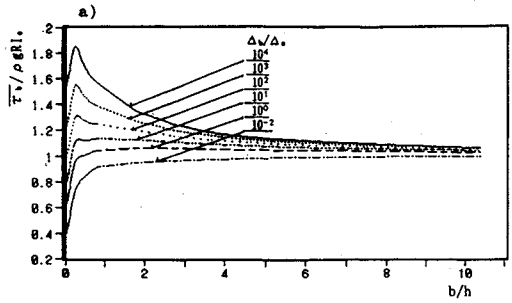

Fig.6(a) Predicted mean bed shear varying with aspect ratio and roughness ratio by Eq.(18).

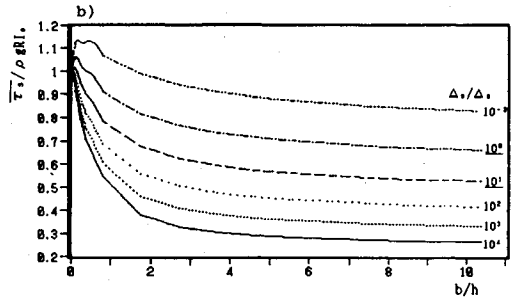

Fig.6(b) Predicted mean side wall shear varying with aspect ratio and roughness ratio by Eq.(18).

Two extreme cases are discussed as follows.

a) If the width becomes much larger, i.e. $b/h\to\infty$, the Eq.(18a) is transformed into,

$$\left.\begin{aligned}\frac{\bar{\tau}}{\tau_0}&=1\\\frac{\bar{\tau}}{\tau_0}&=\frac{z_0}{h}\left(\frac{1}{ln(1+1/\beta)}-\beta\right)\end{aligned}\right\}\cdots\cdots(19)$$

b) If the depth becomes much larger, i.e. $b/h\to 0$, the Eq.(18c) is transformed into,

$$\left.\begin{aligned}\frac{\bar{\tau}_s}{\tau_0}&=1\\\frac{\bar{\tau}_b}{\tau_0}&=\frac{y_0}{b}\left(\frac{1}{ln(1+1/\beta)}-\beta\right)\end{aligned}\right\}\cdots\cdots(20)$$

Fig.6 shows the predicted mean boundary shear varying with the two parameters of aspect ratio and roughness ratio in Eq.(18). When the aspect ratio is very large, $\bar{\tau}_b/\rho gRI_e$ is close to 1 for all roughness ratio, but $\bar{\tau}_s/\rho gRI_e$ is different for varied roughness ratio. When the aspect ratio is very small, the results are just the opposite.

Fig.7 and **Fig.8** are the comparisons of Eq.(18) with experimental data at uniform boundary roughness in channel and duct. While **Fig.9** is the comparison of Eq.(18) with experimental data at non-uniform boundary roughness in open channel. The boundary roughness height for smooth plate obtained in this study is about $\Delta=0.05\sim0.1$ cm. In

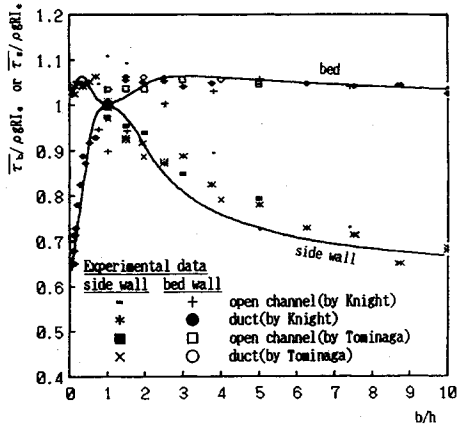

Fig.7 Comparison of calculated mean boundary shear for uniform roughness $\bar{\tau}_b/\rho gRI_e$ or $\bar{\tau}_s/\rho gRI_e$ by Eq.(18) with experimental data by Tominaga[3] & Knight[12),13)].

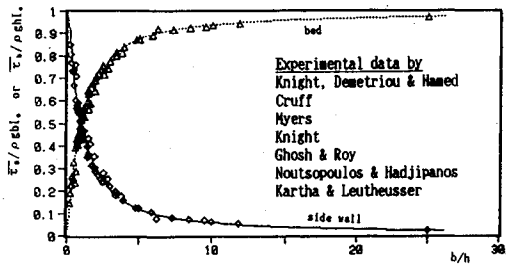

Fig.8 Comparison of calculated mean boundary shear for uniform roughness $\bar{\tau}_b/\rho ghI_e$ or $\bar{\tau}_s/\rho gbI_e$ by Eq.(18) with experimental data by Knight et al.[15], Cruff[16], Myers[18], Knight[14], Ghosh and Roy[11], Noutsopoulos and Hadjipanos[19], Kartha and Leutheusser[17].

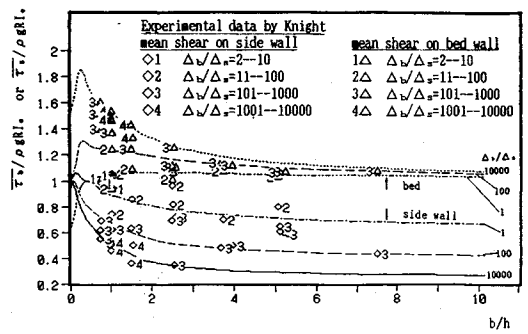

Fig.9 Comparison of calculated mean boundary shear for non-uniform roughness by Eq.(18) with experimental data by Knight et al.[13].

general, the roughness height for smooth wall may be determined by using Moody's results[22].

4. EVALUATION OF VELOCITY DISTRIBUTION

In general, the velocity distribution in open channel has three-dimensional characteristics, which is difficult to analyze theoretically. In order to evaluate the effects of the bed or the side wall, the mean velocity distribution in width or depth direction is discussed individually by using the above results.

For the wide-shallow flow in region II shown in **Fig.4**(a), integrating basic Eq.(6) along depth, we obtain,

$$\rho gI_e z-\frac{1}{h}\int_0^z \tau_b dz-\bar{\tau}_s+(\bar{\tau}_{xz}-\rho\overline{uw})=0 \quad \cdots\cdots(21)$$

where

$$\bar{\tau}_{xz}-\rho\overline{uw}=\frac{1}{h}\int_0^h\left(-\rho\overline{u'w'}+\nu\frac{\partial u}{\partial z}-\rho uw\right)dy$$

According to Boussinesq's assumption,

$$\bar{\tau}_{xz}=\rho\bar{\varepsilon}_{xz}\frac{d\bar{u}}{dz} \quad \cdots\cdots(22)$$

where $\bar{u}$ is depth-averaged velocity, $\bar{u}=\frac{1}{h}\int_0^h u dy$, $\bar{\varepsilon}_{xz}$ is depth-averaged turbulence exchange coefficient, and can be expressed as,

$$\bar{\varepsilon}_{xz}=\kappa_s\bar{u}_{*s}z \quad \cdots\cdots(23)$$

where $\bar{u}_{*s}=\sqrt{\bar{\tau}_s/\rho}$, the coefficient κ_s is determined by experiment.

$\rho\overline{uw}$ representing the depth-averaged momentum transfer in transverse direction is caused by secondary flow, and may be neglected. Thus substituting Eq.(17), Eq.(21) is transformed into,

$$\bar{u}_{*s}\left(1-\frac{\tau_0}{\bar{\tau}_s}\frac{z}{R}\right)+\bar{u}_{*s}\frac{\beta}{ln(1+1/\beta)}\frac{z_0}{R}\left\{ln\left(1+\frac{1}{\beta}\frac{z}{z_0}\right)+\frac{1}{\beta}\frac{z}{z_0}\left[ln\left(1+\frac{1}{\beta}\frac{z}{z_0}\right)-1\right]\right\}=\rho\kappa_s z\frac{d\bar{u}}{dz} \quad \cdots\cdots(24)$$

As the solution is quite complex, some simplification should be made. The latter part of the third term is one order higher of z/z_0 and can be ignored. On the other hand, by using the Prandtl's approximation on shear stress near the wall, i.e. $\{1-y/h\approx 1\}$, the depth-averaged velocity formula can be obtained as,

$$\bar{u}=\bar{u}_{btw0}-\frac{\bar{u}_{*s}}{\kappa_s}\left\{ln\frac{z_0}{z}+\frac{\tau_0}{\bar{\tau}_s}\frac{z_0}{b}\left(1+\frac{h}{b}\right)\right.$$
$$\left.\frac{\beta}{ln(1+1/\beta)}\left[ln\left(1+\frac{1}{\beta}\right)ln\frac{1}{\beta}-ln\left(1+\frac{1}{\beta}\frac{z}{z_0}\right)ln\left(\frac{1}{\beta}\frac{z}{z_0}\right)-\left(1-\frac{z}{z_0}\right)\right\} \quad \cdots\cdots(25a)$$

$$-\left(ln\frac{1}{e\beta}-\beta\right)ln\frac{1+1/\beta}{1+z/\beta z_0}\Big]\Big\} \qquad 0\leqq z\leqq z_0$$

$$\bar{u}=\bar{u}_{btw0} \qquad z_0\leqq z\leqq b$$

where $e=2.71828$, $\bar{u}_{btw0}$ is depth-averaged velocity in region I, and can be determined by the Nikuradse-Prandtl formula.

$$\bar{u}_{btw0}=\frac{\sqrt{\rho ghI_e}}{\kappa}ln\frac{3.35u_*h}{\nu}$$

for smooth region ····(26)

$$\bar{u}_{btw0}=\frac{\sqrt{\rho ghI_e}}{\kappa}ln\frac{11h}{\Delta_b}$$ for rough region ··(27)

in which κ is the Karman constant and $\kappa=0.4$, Δ_b denotes the bed roughness height.

The width-averaged velocity formula for the narrow-deep flow in region II shown in **Fig.4**(b) can also be obtained in the same way.

$$\bar{u}=\bar{u}_{stw0}-\frac{\bar{u}_{*b}}{\kappa_b}\Big\{ln\frac{y_0}{y}+\frac{\tau_0}{\bar{\tau}_b}\frac{y_0}{h}\left(1+\frac{b}{h}\right)\frac{\beta}{ln(1+1/\beta)}\Big[ln\left(1+\frac{1}{\beta}\right)ln\frac{1}{\beta}-ln\left(1+\frac{1}{\beta}\frac{y}{y_0}\right)ln\left(\frac{1}{\beta}\frac{y}{y_0}\right)-\left(1-\frac{y}{y_0}\right)-\left(ln\frac{1}{e\beta}-\beta\right)ln\frac{1+1/\beta}{1+z/\beta z_0}\Big]\Big\} \qquad 0\leqq y\leqq y_0$$

$$\bar{u}=\bar{u}_{stw0} \qquad y_0\leqq y\leqq h$$

····· (25b)

where $\bar{u}_{stw0}$ is width-averaged velocity in region I, and can be determined by the Nikuradse-Prandtl's formula. κ_b is a coefficient determined by experiment.

Fig.10(a) is the comparison of width-averaged velocity distribution by Eq.(25) with experimental data by the authors. Fig.10(b) is the comparison of depth-averaged velocity distribution by Eq.(25) with experimental data by NHRI. The experiment was carried out in a plate flume with 30000 mm in length and 1240 mm in width by the Nanjing Hydraulic Research Institute of China in 1958. The velocity was measured with Pitot tube. **Fig.10**(c) is the comparison of depth-averaged velocity distribution by Eq.(25) with experimental data by Yassin (1953). The velocity was also measured with Pitot tube. These calculated results show that κ_s or κ_b is related to roughness with little variation as given in **Fig.11**.

5. EVALUATION OF FLOW RESISTANCE

The friction factor in open channel flow is generally defined as :

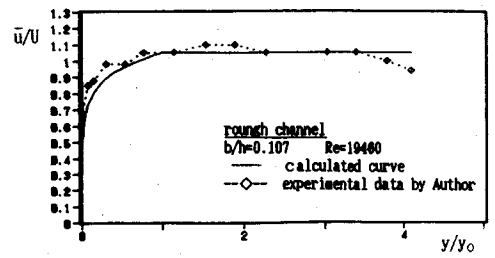

Fig.10(a) Comparison of calculated width-averaged velocity distribution by Eq.(25) with experimental data by the authors.

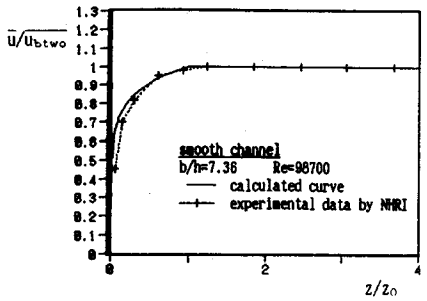

Fig.10(b) Comparison of calculated depth-averaged velocity distribution by Eq.(25) with experimental data by NHRI[10].

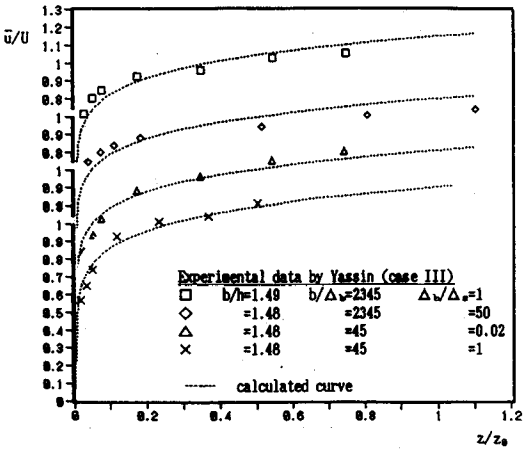

Fig.10(c) Comparison of calculated depth-averaged velocity distribution by Eq. (25) with experimental data by Yassin[6].

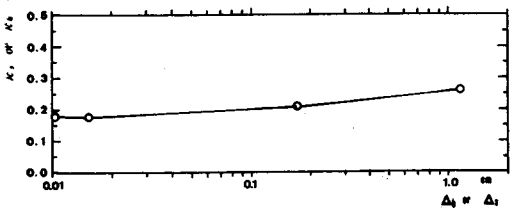

Fig.11 Coefficients κ_s and κ_b.

$$f=2\left(\frac{u_*}{U}\right)^2 \quad \cdots\cdots (28)$$

where u_* is shear velocity, $u_*=\sqrt{gRI_e}$, U is average velocity over the cross section.

The friction factor formula can be got by integrating the velocity distribution formula obtained above.

For wide-shallow flow :

$$U=\frac{1}{b}\int_0^b \bar{u}dz \quad \cdots\cdots (29a)$$

when $b\geq z_0$

$$f=\frac{2}{\left\{\frac{\bar{u}_{btw0}}{u_*}-\sqrt{\frac{\bar{\tau}_s}{\tau_0}}\frac{1}{\kappa_s}\left(\frac{z_0}{b}+0.466\frac{\tau_0}{\bar{\tau}_s}\left(1+\frac{h}{b}\right)\left(\frac{z_0}{b}\right)^2\right)\right\}^2} \quad \cdots\cdots (30a)$$

when $b\leq z_0$

$$f=2/\left\{\frac{\bar{u}_{btw0}}{u_*}-\sqrt{\frac{\bar{\tau}_s}{\tau_0}}\frac{1}{\kappa_s}\left[1+ln\frac{z_0}{b}+0.03\frac{\tau_0}{\bar{\tau}_s}\frac{z_0}{b}\left(1+\frac{h}{b}\right)\left(1.824\frac{z_0}{b}+0.5\frac{b}{z_0}+1.46\,ln\left(1+12.66\frac{b}{z_0}\left(1+0.079\frac{z_0}{b}\right)-4.89\right)\right)\right]\right\}^2 \quad \cdots\cdots (30b)$$

If the width becomes much larger, i.e. $b/h\rightarrow\infty$, then

$$f=\frac{2}{\left(\frac{\bar{u}_{btw0}}{u_*}\right)^2} \quad \cdots\cdots (31)$$

It is the resistance formula of two-dimensional flow.

For narrow-deep flow :

$$U=\frac{1}{h}\int_0^h \bar{u}dy \quad \cdots\cdots (29b)$$

when $h\geq y_0$

$$f=\frac{2}{\left\{\frac{\bar{u}_{stw0}}{u_*}-\sqrt{\frac{\bar{\tau}_b}{\tau_0}}\frac{1}{\kappa_b}\left(\frac{y_0}{h}+0.466\frac{\tau_0}{\bar{\tau}_b}\left(1+\frac{b}{h}\right)\left(\frac{y_0}{h}\right)^2\right)\right\}^2} \quad \cdots\cdots (30c)$$

when $h\leq y_0$

$$f=2/\left\{\frac{\bar{u}_{stw0}}{u_*}-\sqrt{\frac{\bar{\tau}_b}{\tau_0}}\frac{1}{\kappa_b}\left[1+ln\frac{y_0}{h}+0.03\frac{\tau_0}{\bar{\tau}_b}\frac{y_0}{h}\left(1+\frac{b}{h}\right)\left(1.824\frac{y_0}{h}+0.5\frac{h}{y_0}+1.46\,ln\left(1+12.66\frac{h}{y_0}\left(1+0.079\frac{y_0}{h}\right)-0.489\right)\right)\right]\right\}^2 \quad \cdots\cdots (30d)$$

If the depth becomes much larger, i.e. $b/h\rightarrow 0$, then

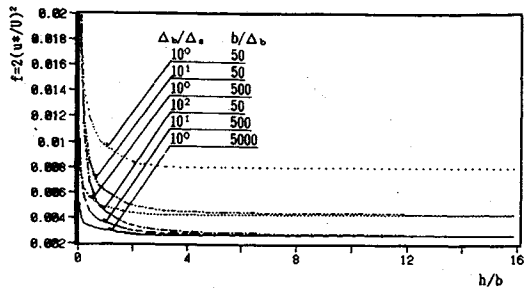

Fig.12(a) Predicted friction factor in $\Delta_b/\Delta_s\geq 1$ by Eq.(30).

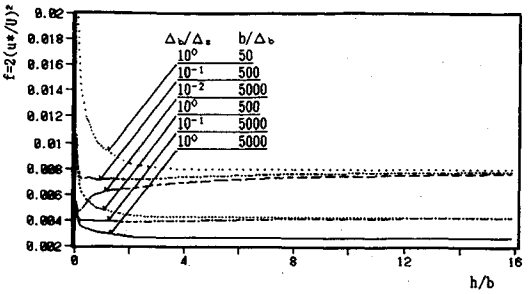

Fig.12(b) Predicted friction factor in $\Delta_b/\Delta_s\leq 1$ by Eq.(30).

$$f=\frac{2}{\left(\frac{\bar{u}_{stw0}}{u_*}\right)^2} \quad \cdots\cdots (32)$$

It is also the resistance formula of two-dimensional flow.

All coefficients in Eq.(30) are calculated when $\beta=0.079$.

Fig.12(a) is the friction factor varying with aspect ratio and roughness ratio when $\Delta_b/\Delta_s\geq 1$ according to Eq.(30). **Fig.12**(b) is the friction factor varying with aspect ratio and roughness ratio when $\Delta_b/\Delta_s\leq 1$ according to Eq.(30).

Fig.(13a-13d) are the comparisons of Eq.(30) with experimental data by Knight[14] and Yassin[6].

6. CONCLUSIONS

Some conclusions can be made from this study as follows :

(1) A flow pattern has been proposed, in which open channel flow is divided into two types according to aspect ratio and roughness ratio, one is the wide-shallow flow mainly depending upon the bed, while the other is the narrow-deep flow mainly depending on the side wall.

(2) An experiment conducted with an aspect ratio of 0.107 shows that the velocity distribution normal to the side wall agrees with the Nikuradse-Prandtl's logarithmic law, and the boundary shear stress on the side wall is $\tau_s=\rho gbI_e$ except in the

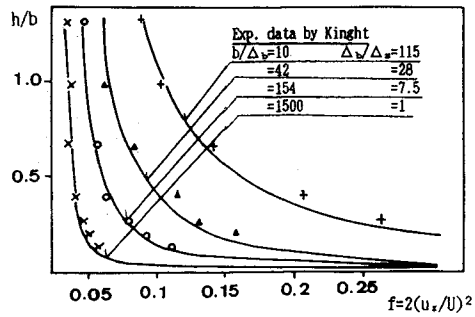

Fig.13(a) Comparison of calculated friction factor by Eq.(30) with experimental data by Knight[14].

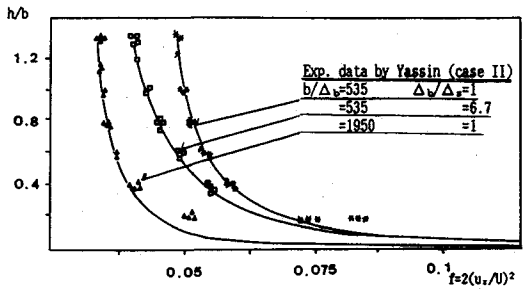

Fig.13(c) Comparison of calculated friction factor by Eq.(30) with experimental data by Yassin (Run Ⅱ)[6].

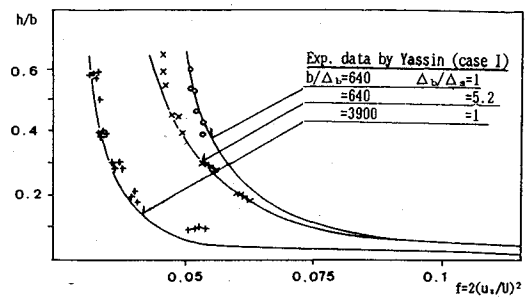

Fig.13(b) Comparison of calculated friction factor by Eq.(30) with experimental data by Yassin (Run Ⅰ)[6].

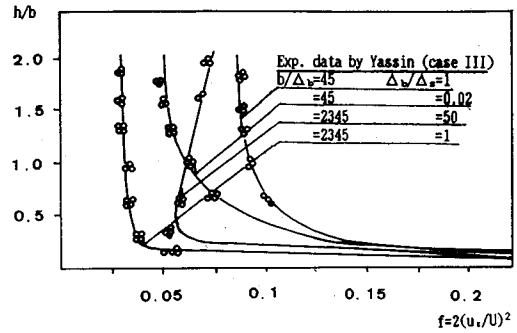

Fig.13(d) Comparison of calculated friction factor by Eq.(30) with experimental data by Yassin (Run Ⅲ)[6].

regions near the water surface and the bed.

(3) The range influenced by the side wall is related to aspect ratio and roughness ratio, and can be estimated by Eq.(10). The critical value of width-depth ratio to distinguish wide-shallow flow from narrow-deep flow is given by Eq.(12).

(4) The distributions of boundary shear on the bed and the side wall are similar on condition that the influence of water surface is neglected, and are given by Eq.(17). The mean boundary shear stress can be evaluated with Eq.(18). The relationships of the boundary shear with aspect ratio and roughness ratio are shown in **Fig.**(6a, 6b).

(5) The velocity distribution in the cross section depending on the boundary shear on both the bed and the side wall can be calculated by Eq.(25).

(6) The friction factor is obtained as Eq.(30). The friction factor varying with aspect ratio and roughness ratio are shown in **Fig.12**.

(7) The results obtained in this paper have been verified by a wide range of experimental data. The comprehensive agreement is quite evident. The present results can be used to evaluate the effect of the side wall upon hydraulic model experiments, to calculate bed shear associated with sediment transport, to estimate the shear stress on the river banks and etc..

REFERENCE

1) Chiu, C.L., Hsiung, D.E. and Lin, H.C. : Three-Dimensional Open Channel Flow, Journal of the Hydraulics Division, ASCE, Vol.104, No.HY8, Proc. Paper 13963, pp.1119~1136, Aug., 1978.

2) Nezu, I. and Nakagawa, H. : Investigation on Three-Dimensional Turbulent Structure in Uniform Open-Channel and Closed Duct Flow, Proc. of JSCE, No.369, pp.89~98, 1985 (Japanese).

3) Tominaga,A. & Ezaki,K. : An Experiment Study on Three-Dimensional Turbulent Structure in A Rectangular Open Channel Flow, Proc. of JSCE, No.357, 1985 (in Japanese).

4) Kimura, K. : An Approximate Analysis of Flow Through Rectangular Channel, Proc. of JSCE, No.251, pp.45~57, 1976 (in Japanese).

5) Egashira, S., Kuroki, M., Sawai, K. and Yamasaka, M. : Methods of Evaluate the Bed Shear Stress in Open Channel Flow, Proc. of the 32 th Japanese Conference on Hydraulics, pp.821~826,1988 (in Japanese).

6) Yassin,A. : Mean Roughness Coefficient in Open Channel with Different Roughness of Bed and Side Walls, Verlag Leemann Zurich.

7) Daido, A. : An Effect of Aspect Ratio and Roughness on the Wall Shear Stress of Open Channel, Proc. of the 29 th Japanese Conference on Hydraulics, pp.821～826, 1985 (in Japanese).
8) Yang, Y.D. : Resistance Computation of Open Channel Flow with Nonhomogeneous Boundary, Jour. of Nanjing Hyd. Res. Ins., No.3, pp.58～68, 1989 (in Chinese).
9) Yang, Y.D. : Approach to Resistance Coefficient of Flow in Rectangular Flumes, Jour. of Nanjing Hyd. Res. Ins., No.3, Sept. pp.59～69, 1984 (in Chinese).
10) Yang, Y.D. and Daido, A. : Evaluation on Open Channel Flow with Varying Aspect Ratio, Proc. of Inter.Symp. on Hyd. Res. in Nature and Lab., Nov. 1992 (Wuhan, China).
11) Ghosh, S.N. and Roy, N. : Boundary Shear Distribution in Open Channel Flow, Journal of Hydraulics Division, ASCE, Vol.96, No.HY4, Proc. Paper 7241, pp.967～994, Apr., 1970.
12) Knight, D.W. and Patel, H.K.S. : Boundary Shear in Smooth Rectangular Ducts, Journal of Hydraulics Engineering, ASCE, Vol.111, No.1, Jan., 1985.
13) Knight, D.W. : Boundary Shear in Smooth and Rough Channels, Journal of the Hydraulics Division, ASCE, Vol.107, No.HY7, Proc. Paper 16364, July, pp.839～851, 1981.
14) Knight, D.W. & Macdonald, J.A. : Open Channel Flow with Varying Bed Roughness, Journal of the Hydraulics Division, ASCE, Vol.105, No. HY9 Proc. Paper 14839, pp.1167～1183, Sept. 1979.
15) Knight, D.W., Demetriou, J.D. and Hamed, M.E. : Boundary Shear in Smooth Rectangular Channels, Journal of Hydraulics Division, ASCE, Vol.110, No.4, Proc. Paper 18744, Apr., pp.405～422, 1984.
16) Cruff, R.W. : Cross-Channel Transfer of Linear Momentum in Smooth Rectangular Channels, Water- Supply Paper 1592-B, United States Geological Survey, pp.B1～b26, 1965.
17) Kaetha, V.C. and Leutheusser, H.J. : Distribution of Tractive force in Open Channels, Journal of the Hydraulics Division, ASCE, Vol.96, No.HY7, Proc. Paper 7415, pp.1469～1483, July, 1970.
18) Myers, W.R.C. : Flow Resistance in Wide Rectangular Channels, Journal of the Hydraulics Division, ASCE, Vol.108, No.HY4, Proc. Paper 17008, Apr, pp.471～482, 1982.
19) Noutsopoulos, G.C. and Hadjipanos, P.A. : Discussion of boundary shear in smooth and rough channels, by Knight, D.W., Jour. of the Hyd. Divi.,ASCE, Vol.108,No.Hy6, pp.809～812, June, 1982.
20) Sawano, K. et al. : Hydraulic Research for Revetments, Proc. of the 31 th Japanese Conference on Hydraulics, pp.395～400, 1987 (in Japanese).
21) Hojyo, K., Shimizu, Y. and Itakura, I. : Calculation of Boundary Shear Stress in Open Channel Flow, Proc. of the 34 th Japanese Conference on Hydraulics, pp.421～426, 1990. (in Japanese).
22) Moody, L.F. : Friction Factors for Pipe Flow, Tran. ASME, pp.671, 1944.
23) Einstein, H.A. : Method of Calculating the Hydraulic Radius in a Cross Section with Different Roughness, Tran. ASCE, Vol.107, pp.575～577, 1942.

(Received, April 30, 1992)

アスペクト比および壁面の粗さ比が流れに及ぼす影響の評価

楊永荻・大同淳之

本論文では，開水路におけるアスペクト比（半水路幅／水深）および底面と側面の粗さ比の変化に対応する流れモデルを構築し，これをもとに壁面せん断力分布を考察した．それに基づいて，壁面平均せん断力，流速分布及び流水抵抗係数とアスペクト比および壁面の粗さ比との関係をそれぞれ検討した．提案した評価式はアスペクト比および壁面の粗さ比の広い範囲に適合し，既往の実験値と比較したとき，良好な一致を示した．

土木学会新刊案内

BASIC Pascal C
による土木情報処理の基礎 II (FD付き)

土木情報システム委員会　　B5版　271ページ　定価 3,800円
教育問題小委員会編　　会員特価 3,400円　(〒350)

●本書は，次のような方針で編集されています．

- 卒業研究などで研究室に出入りを始めた学生や，パソコンなどを使用する実務現場に配属された技術者などが，自ら学習しようとするときに役立つテキストとする．
- 例題は，建設分野に関係のある学生や技術者に親しみやすい内容とする．
- すべての例題(全37題)について，パソコン上で動作する4言語(N88-BASIC(MS-DOS版),Quick BASIC, Turbo Pascal, Turbo C) でのプログラム例を，できるだけ同じアルゴリズムで作成して示す．また，プログラム中に詳細なコメントを記述し，読者の理解を助ける．
- すべてのプログラムは，その入力データと共に付属のフロッピーディスク(5.25in)に収録して提供する．
- 巻末付録には，今回対象とした4言語とFORTRAN 77の文法照表を示し，各言語間の相違点を示す．

●本書の構成要素の概要は次の通りです。

本書は，学校や企業の研究室・実験室などで頻繁に発生するデータのハンドリングやアプリケーションプログラムへの入力データの仕様変更，出力からのデータ抽出・グラフ化などの作業を，気軽にコンピュータを使用して行える素養や能力を自ら習得しようとする方々へのよい参考書となると考えていますので，広くご利用ください。

■お申込は土木学会刊行物販売係へ
〒160 東京都新宿区四谷1丁目無番地　土木学会　電話03-3355-3441　内線144・145・146　振替東京6-16828
FAX03-3355-3446

地下水変動解析プログラム(V-2)

未来設計企業
CRC

あの地下水解析ソフトがさらに機能充実!

UNISSF ユニセフ(V-2)

スピーディな同定・安価な解析

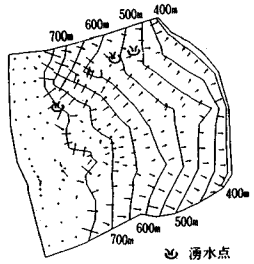

初期状態の地下水流

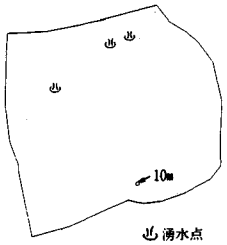

トンネル掘削開始直後

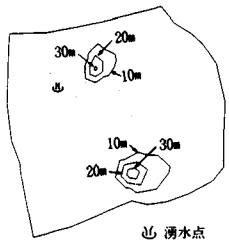

約4日後

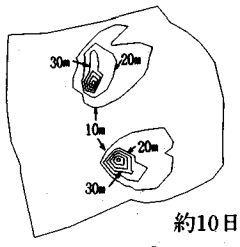

約10日後

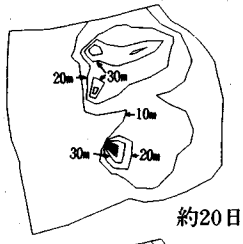

約20日後

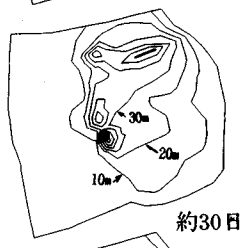

約30日後

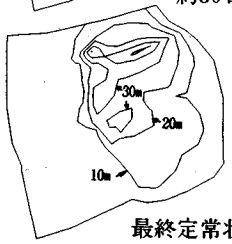

最終定常状態

特長

○有限要素法による準3次元解析を中心とした
地下水の流れのトータルシステムです。

○観測水位と計算水位より、非線形最小二乗法を用いて
帯水層定数の同定が可能です。(逆解析手法)

○建設・土木工事（掘削・ディープウェルその他）の
解析に対応する多くの機能を備えています。

○メッシュ・ジュネレータにより、
モデル（要素分割）作成の手間を軽減できます。

○図化処理プログラムにより、
結果の確認が容易に行えます。

適応機種：SUN, NEWS, HP,
IBM 30XX, FACOM-Mシリーズ 他

このシステムは、情報処理振興事業協会の委託を受けて開発したものです。

IPA 情報処理振興事業協会

株式会社CRC総合研究所 西日本支社

問合せ先
〒541 大阪市中央区久太郎町4丁目1-3
(06) 241-4121 営業担当:岩 崎
(03)3665-9741 本社窓口:菅 原

土と水の連成逆解析プログラム

未来設計企業 CRC

UNICOUP

応力解析と浸透解析がドッキングした!

軟弱地盤の解析に!

海洋開発・埋立

盛土・掘削

出力項目

- ●各節点での変位、各要素での応力
- ●各節点での全水頭・圧力水頭 他
- ●豊富な図化処理
  変位図、変位ベクトル図、応力ベクトル図、応力コンター図、安全率コンター図、水頭コンター図、圧力水頭コンター図

プログラムの特長

- ●応力と地下水の流れをカップルさせた問題が解析可能です。(圧密含む)
- ●地下水の流れは飽和・不飽和域を対象としています。
- ●多段掘削・盛土や降雨等が扱えます。
- ●梁や連結要素も扱え実用的です。
- ●経時観測記録(変位・水位)があれば、非線形最小二乗法に基づき変形係数や透水係数が逆解析できます。(順解析、逆解析がスイッチにて選択可能です。)
- ●弾性・非線形弾性・弾塑性・弾粘塑性を示す地盤が扱えます。
  非線形弾性(電中研式、ダンカン・チャンの双曲線モデル)
  弾塑性(ドラッガー・プラガー、モール・クーロン、カムクレイモデル、ハードニング、ソフトニング)
  弾粘塑性(関口・太田モデル)

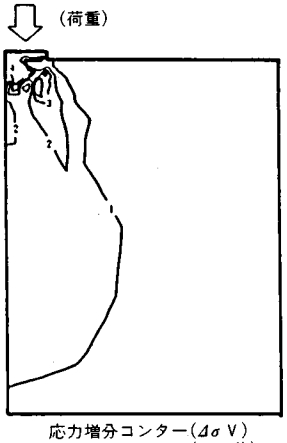

応力増分コンター($\Delta\sigma$ V)
(10日後)

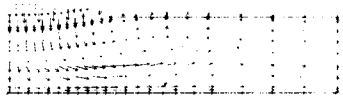

変位ベクトル図 (40日後)

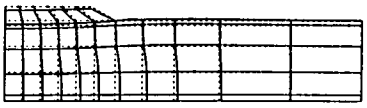

盛土(40日)後の地盤の変形

盛土(40日)後の地下水の流れと水頭コンターおよび自由水面

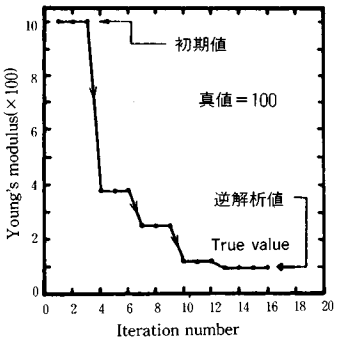

ヤング率と繰り返し回数の関係

逆解析によるパラメータの推定

このシステムは、情報処理振興事業協会の委託を受けて開発したものです。

IPA 情報処理振興事業協会

株式会社CRC総合研究所 西日本支社

問合せ先
〒541 大阪市中央区久太郎町4丁目1-3
(06) 241-4121 営業担当:岩 崎
(03)3665-9741 本社窓口:菅 原

土木学会論文集

昭和二十七年五月二十八日 第三種郵便物認可
平成五年五月十五日・印刷
平成五年五月二十一日・発行
土木学会論文集 毎月二回二十日・二十一日発行

定価 一、〇〇〇円(本体価格・九七一円)